RSC Advances

PAPER

View Article Online
View Journal | View Issue

Cite this: *RSC Adv.*, 2021, **11**, 35011

Oxazolomycins produced by *Streptomyces glaucus* and their cytotoxic activity†

Yu Mu,‡[a] Yi Jiang,‡*[b] Xiaodan Qu,[a] Bo Liu,[a] Junfeng Tan,[a] Guiding Li,[b] Mingguo Jiang,*[c] Liya Li,[a] Li Han[a] and Xueshi Huang*[a]

Received 16th August 2021
Accepted 16th October 2021

DOI: 10.1039/d1ra06182h

rsc.li/rsc-advances

Six oxazolomycins (**1–6**) were isolated from the fermentation broth of a soil-borne bacterial strain, *Streptomyces glaucus*. The structures of the new compounds, oxazolomycins D–F (**1–3**) and glaucumycins A, B (**6a**/**6b**), were elucidated by detailed spectroscopic data analysis. Oxazolomycins **1**, **2**, **4**, and **5** demonstrated weak or modest cytotoxic activities against four human cancer cell lines, with IC_{50} values ranging from 10.6 ± 1.7 to 89.5 ± 6.6 μM (or >100 μM). Further study showed that **4** caused S phase cell cycle arrest in SMMC7721 cells through down-regulating the protein expression of cyclin A2, CDK2. Meanwhile, **4** induced apoptosis in SMMC7721 cells through down-regulating the protein levels of Bcl-2, up-regulating the levels of Bax, and activating the cleavage of caspase-3.

1. Introduction

Oxazolomycin and its congeners are a relatively rare family of natural products produced by streptomycetes.[1,2] The common structural characteristics of this class of compounds contain a unique spiro fused β-lactone-γ-lactam core and a terminal oxazole ring, and these two structural moieties are linked by a triene and an (*E*,*E*)-diene aliphatic chain.[1,2] Natural sources of oxazolomycins are extremely rare, and only fifteen members, including neooxazolomycin,[3] oxazolomycins A, B, C,[4,5] curromycins A, B (also known as triedimycins A, B),[6,7] 16-methyl oxazolomycin,[8,9] KSM-2690 B, KSM-2690 C,[10] lajollamycins,[11,12] bisoxazolomycin A, and oxazolomycin A2 (ref. 13) have been found up to this point, and all of them were isolated from *Streptomyces* spp. Furthermore, several oxazolomycin related compounds, inthomycins and phthoxazolins, which only possess the oxazole ring and a triene fragment were also reported.[14,15] The oxazolomycins showed a wide range of biological activities, *e.g.* oxazolomycin A, neooxazolomycin, curromycin A, 16-methyl oxazolomycin, KSM-2690 B, KSM-2690 C, lajollamycin, bisoxazolomycin A, and oxazolomycin A2 displayed cytotoxic activity;[2] oxazolomycin A, curromycin A, 16-methyl oxazolomycin, KSM-2690 B, lajollamycin, bisoxazolomycin A, and oxazolomycin A2 exhibited antibacterial activity mainly against Gram-positive bacteria;[2] oxazolomycin A showed antiviral activity against influenza A, herpes simplex, and vaccinia;[1,2] oxazolomycins A, B, C and curromycins A, B inhibited crown gall formation on potato tubers.[16–18] The unique structure and multiple biological activities of oxazolomycins has attracted much attention from organic chemists. The total synthesis of neooxazolomycin,[19,20] oxazolomycin A,[21] and lajollamycin[22] has been accomplished. In addition, several synthesis method to establish the different structural segments of oxazolomycins have been reported.[23–27]

In our continuous search for bioactive natural compounds from microbial sources, the secondary metabolites of a soil-borne *Streptomyces glaucus* (YIM 33872) were investigated. *Streptomyces glaucus* was isolated from the soil sample collected from the rainforest of Xishuangbanna, Yunnan, China. A small scale (100 mL) fermentation broth of *S. glaucus* showed diversiform chemical constituents illustrated through HPTLC and HPLC-MS analysis. Chromatographic separation of an EtOAc extract of a large scale fermentation broth of *S. glaucus* led to the isolation of six oxazolomycins, including four new compounds, oxazolomycins D–F (**1–3**), and a pair of isomers, named as glaucumycins A and B (**6a**/**6b**), as well as two known congeners KSM-2690 B and C (**4–5**) (Fig. 1).[9] The structures of new compounds oxazolomycins D–F (**1–3**) and glaucumycins A, B (**6a**/**6b**) were elucidated by extensive spectroscopic data analysis as well as UV, IR, and MS spectra. The cytotoxic effects of **1**, **2**, **4**, **5** were evaluated in four human carcinoma cell lines. The apoptosis and cell cycle arrest of **4** in SMMC7721 cell lines were also investigated. Herein, we report the fermentation, isolation, structural elucidation, and cytotoxic activity of oxazolomycins **1–6**.

[a]*Institute of Microbial Pharmaceuticals, College of Life and Health Sciences, Northeastern University, Shenyang 110819, China. E-mail: huangxs@mail.neu.edu.cn; Fax: +86-24-83656106; Tel: +86-24-83656106*

[b]*Yunnan Institute of Microbiology, Yunnan University, Kunming 650091, China. E-mail: jiangyi@ynu.edu.cn; Fax: +86-871-65173878; Tel: +86-871-65034073*

[c]*Guangxi Key Laboratory for Polysaccharide Materials and Modifications, School of Marine Sciences and Biotechnology, Guangxi University for Nationalities, Nanning 530008, China. E-mail: mzxyjiang@gxun.edu.cn; huangxs@mail.neu.edu.cn; Fax: +86-771-3267023; Tel: +86-771-3267023*

† Electronic supplementary information (ESI) available: 1D and 2D NMR, HRMS spectra for compounds **1–3**, **6** (PDF). See DOI: 10.1039/d1ra06182h

‡ These authors contributed equally to this work.

2. Materials and methods

2.1. General experimental procedures

Optical rotation were determined using an Anton Paar MCP200 automatic polarimeter (Graz, Austria). Ultraviolet spectra were obtained with a Beckman Coulter DU 730 nucleic acid/protein analyzer. IR spectra were recorded with a Bruker Tensor 27 FT-IR spectrometer. ESI-MS were recorded on an Agilent 1290–6420 Triple Quadrupole LC-MS spectrometer (Santa Clara, CA, USA). HRESI-MS experiments were performed using a Bruker Micro TOF-Q mass spectrometer (Bruker Daltonics, Billerica, MA). NMR spectra were recorded on a Bruker Advance III-600 MHz spectrometer (Bruker, Rheinstetten, Germany). Flow cytometric analysis were conducted on an LSR-Fortessa flow cytometer (BD, Franklin Lakes, NJ, USA). MTT and protein quantification were analyzed by a microplate reader (BioTek Synergy H1, BioTek Instruments, Inc., Vermont, USA). Silica gel (100–200 mesh, 200–300 mesh, Qingdao Marine Chemical, Ltd., Qingdao, China), MCI gel (CHP-20P, Mitsubishi Chemical Corp., Tokyo, Japan), and YMC*GEL ODS-A (S-50 μm, 12 nm) (YMC Co., Ltd., Kyoto, Japan) were used for column chromatography. The primary antibodies for cyclin A2, CDK2, p21, Bax, Bcl-2, caspase-3, GAPDH, and horse-radish peroxidase (HRP)-conjugated secondary antibodies were purchased from Cell Signaling Technology (Dancers, MA, USA).

2.2. Microbial material

The producing organism was isolated from a rainforest soil sample collected in Xishuangbanna, Yunnan Province, China. The strain was assigned to be *Streptomyces glaucus* based on morphological characteristics and 16S rRNA gene sequences. The Blast result showed that the sequence was identical (100%) to the sequence of *S. glaucus* LMG 19902 (T) (GenBank accession no. AJ787332). The strain (No. YIM 33872) was deposited in Yunnan Institute of Microbiology, Yunnan University, China.

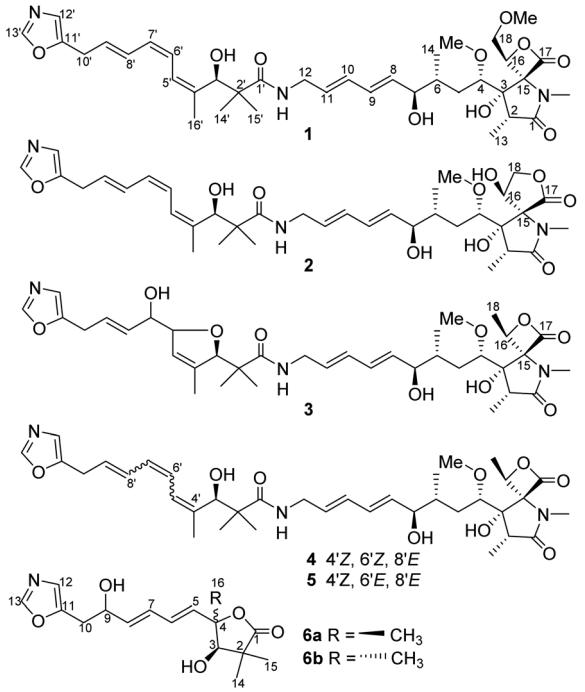

Fig. 1 Structures of compounds **1–6**.

2.3. Fermentation, extraction, and isolation

A slant culture of *S. glaucus* was inoculated into 500 mL Erlenmeyer flasks each containing 100 mL of seed medium composed of 4 g L^{-1} yeast extract, 4 g L^{-1} glucose, 5 g L^{-1} malt extract, 3.75 mg L^{-1} multiple vitamins solution (thiamine 0.5 mg, riboflavin 0.5 mg, niacin 0.5 mg, pyridoxine 0.5 mg, inositol 0.5 mg, calcium pantothenate 0.5 mg, *p*-aminobenzoic acid 0.5 mg, biotin 0.25 mg), and 1 mL L^{-1} trace element solution (2 g L^{-1} $FeSO_4 \cdot 7H_2O$, 1 g L^{-1} $MnCl_2 \cdot 4H_2O$, 1 g L^{-1} $ZnSO_4 \cdot 7H_2O$). The pH was 7.2 with no adjustment, and the flasks were incubated for 2 days at 28 °C on a rotary shaker at 180 rpm. The seed culture was used to inoculate the fermentation medium with 10% volume. The large-scale fermentation was carried out in 1000 mL/2000 mL Erlenmeyer flasks with 200 mL/400 mL of fermentation medium containing soybean meal 10 g L^{-1}, peptone 2 g L^{-1}, glucose 20 g L^{-1}, soluble starch 5 g L^{-1}, yeast extract 2 g L^{-1}, NaCl 4 g L^{-1}, K_2HPO_4 0.5 g L^{-1}, $MgSO_4 \cdot 7H_2O$ 0.5 g L^{-1}, $CaCO_3$ 2 g L^{-1}, with a pH of 7.8 with no adjustment, and the flasks were incubated for 7 days at 28 °C on a rotary shaker at 180 rpm.

The 120 L fermentation broth was collected and clarified with a centrifuge to obtain a culture supernatant. Then, the supernatant was extracted with EtOAc three times. The combined EtOAc extracts were concentrated *in vacuo* to yield 32.7 g dried extract. The total extract was subjected to open silica gel (100–200 mesh) column chromatography with a CH_2Cl_2–MeOH solvent system (from 100 : 1, 50 : 1, 20 : 1, 5 : 1, and 1 : 1 at last) to yield seven fractions. Fraction 3 was subjected to silica gel (200–300 mesh) column chromatography (petroleum ether–EtOAc 1 : 1) to yield three subfractions (Fr.3.1–Fr.3.3). Fr.3.3 was further separated by ODS column chromatography and eluted with MeOH–H_2O (60 : 40) to afford compound **4** (30.6 mg). Fraction 4 was subjected to an ODS column chromatography eluting with MeOH–H_2O (60 : 40) to afford four subfractions (Fr.4.1–Fr.4.4). Fr.4.2 was further separated by silica gel (200–300 mesh) column chromatography (petroleum ether–EtOAc 1 : 1) to give compounds **2** (6.7 mg) and **6** (3.9 mg). Fr.4.3 was separated by silica gel (200–300 mesh) column chromatography (petroleum ether–EtOAc 1 : 1) to give compound **3** (6.5 mg). Fr.4.4 was separated by silica gel (200–300 mesh) column chromatography (petroleum ether–EtOAc 1 : 1) to give compound **1** (7.1 mg). Fr.5 was subjected to a MCI gel CHP-20P column and eluted with MeOH–H_2O (from 0 : 100–100 : 0) to yield five subfractions (Fr.5.1–Fr.5.5). Fr.5.5 was separated by ODS column chromatography eluting with MeOH–H_2O (60 : 40) and further purified by silica gel (200–300 mesh) column chromatography (petroleum ether–EtOAc 1 : 1) to give compound **5** (8.2 mg).

Oxazolomycin D (**1**): yellow oil; $[\alpha]_D^{20} = 97.3$ (*c* 0.37, MeOH); UV (MeOH) λ_{max} (log ε) 232 (4.47), 274 (4.31) nm; IR (film) ν_{max} 3344, 2929, 1820, 1677, 1553, 1458, 1385, 1262, 1093, 1051, 1026, 997 cm^{-1}; ^1H and ^{13}C NMR see Table 1; HRESIMS *m*/*z*: 700.3738 $[M + H]^+$ (calcd for $C_{37}H_{54}N_3O_{10}^+$, 700.3804).

Oxazolomycin E (**2**): yellow oil; $[\alpha]_D^{20} = 59.3$ (*c* 0.27, MeOH); UV (MeOH) λ_{max} (log ε) 232 (4.22), 274 (4.22) nm; IR (film) ν_{max} 3367, 2928, 1765, 1680, 1532, 1455, 1396, 1287, 1205, 1099, 1049, 1026, 999 cm^{-1}; ^1H and ^{13}C NMR see Table 1; HRESIMS *m*/*z*: 684.3500 $[M - H]^-$ (calcd for $C_{36}H_{50}N_3O_{10}^-$, 684.3502).

Oxazolomycin F (**3**): yellow oil; $[\alpha]_D^{20} = 36.5$ (*c* 0.15, MeOH); UV (MeOH) λ_{max} (log ε) 236 (4.06) nm; ^1H and ^{13}C NMR see Table 1; HRESIMS *m*/*z*: 708.3462 $[M + Na]^+$ (calcd for $C_{36}H_{51}N_3NaO_{10}^+$, 708.3467).

Glaucumycins A and B (**6a**/**6b**): colorless oil; UV (MeOH) λ_{max} (log ε) 232 (4.07) nm; IR (film) ν_{max} 3367, 2979, 1756, 1511, 1384, 1278, 1223, 1089, 1025 cm^{-1}; ^1H and ^{13}C NMR see Table 2; HRESIMS *m*/*z*: 330.1315 $[M + Na]^+$ (calcd for $C_{16}H_{21}NNaO_5^+$, 330.1312).

2.4. Cytotoxicity assay

The cytotoxicities of **1–2**, **4–6** were evaluated against four human cancer cell lines including a gastric carcinoma cell line

Table 1 ^1H NMR (600 MHz) and ^{13}C NMR (150 MHz) data for compounds **1–3** in DMSO-d_6

	1		**2**		**3**	
Position	δ_C, mult.	δ_H, mult. (*J* in Hz)	δ_C, mult.	δ_H, mult. (*J* in Hz)	δ_C, mult.	δ_H, mult. (*J* in Hz)
1	174.6, C		175.9, C		174.8, C	
2	43.7, CH	2.37, q (7.3)	42.9, CH	2.42, q (7.5)	44.0, CH	2.36, q (7.3)
3	81.3, C		86.1, C		81.1, C	
4	83.1, CH	3.33, overlapped	81.8, CH	3.15, overlapped	83.0, CH	3.35, t (4.6)
5	32.3, CH_2	1.96, dt (16.0, 6.5)	32.8, CH_2	1.96, dt (16.6, 4.6)	32.4, CH_2	1.94, dt (15.2, 5.2)
		1.12, m		1.10, m		1.13, m
6	37.2, CH	1.59, m	38.2, CH	1.52, m	37.1, CH	1.60, m
7	75.7, CH	3.83, m	75.6, CH	3.79, q (5.8)	75.5, CH	3.82, q (5.6)
8	134.9, CH	5.60, m	135.1, CH	5.60, m	134.8, CH	5.59, dd (14.3, 4.7)
9	130.3, CH	6.11, m	130.2, CH	6.12, m	130.2, CH	6.11, m
10	130.7, CH	6.12, m	130.7, CH	6.12, m	130.6, CH	6.11, m
11	130.4, CH	5.61, m	130.4, CH	5.61, m	130.3, CH	5.61, m
12	40.9, CH_2	3.71, m	40.5, CH_2	3.72, m	40.7, CH_2	3.68, dt (15.8, 5.6)
						3.73, dt (15.8, 5.6)
13	10.2, CH_3	1.03, d (7.5)	11.1, CH_3	1.06, d (7.5)	10.2, CH_3	1.03, d (7.5)
14	16.5, CH_3	0.86, d (6.6)	16.8, CH_3	0.86, d (6.6)	16.4, CH_3	0.86, d (6.8)
15	85.6, C		71.6, C		83.9, C	
16	79.4, CH	4.95, dd (9.1, 2.4)	69.9, CH	4.83, m	77.7, CH	4.95, q (6.6)
17	170.7, C		173.7, C		170.5, C	
18	72.0, CH_2	4.13, dd (12.0, 9.1)	69.1, CH_2	4.40, t (7.9)	17.2	1.70, d (6.5)
		3.99, dd (12.0, 2.4)		4.17, t (7.9)		
1′	176.5, C		176.5, C		175.2, C	
2′	46.3, C		46.4, C		46.4, C	
3′	73.5, CH	4.64, d (4.6)	73.5, CH	4.63, d (4.8)	91.7, CH	4.78, d (5.7)
4′	140.4, C		140.4, C		138.4, C	
5′	123.9, CH	6.41, d (12.0)	123.9, CH	6.41, d (11.9)	124.1, CH	5.47, brs
6′	124.9, CH	6.32, t (11.3)	124.9, CH	6.32, t (11.9)	88.5, CH	4.51, brs
7′	127.6, CH	5.93, t (11.3)	127.6, CH	5.93, t (11.9)	73.7, CH	3.89, q (5.3)
8′	128.5, CH	6.75, dd (14.5, 11.3)	128.5, CH	6.75, dd (14.6, 11.9)	133.5, CH	5.53, dd (15.4, 5.3)
9′	129.4, CH	5.79, dt (14.5, 7.0)	129.5, CH	5.79, dt (14.6, 7.0)	125.5, CH	5.68, dt (15.4, 6.4)
10′	28.7, CH_2	3.55, d (7.0)	28.7, CH_2	3.55, d (7.0)	28.1, CH_2	3.40, d (6.4)
11′	150.9, C		151.0, C		151.3, C	
12′	122.5, CH	6.90, s	122.5, CH	6.90, s	122.3, CH	6.83 s
13′	151.8, CH	8.24, s	151.8, CH	8.25, s	151.6, CH	8.21, s
14′	25.2, CH_3	1.09, s	25.2, CH_3	1.10, s	24.5, CH_3	1.11, s
15′	22.0, CH_3	0.97, s	22.0, CH_3	0.97, s	18.7, CH_3	0.93, s
16′	20.4, CH_3	1.75, s	20.5, CH_3	1.73, s	14.0, CH_3	1.55, s
4-OCH_3	56.2, CH_3	3.14, s	56.2, CH_3	3.11, s	56.3, CH_3	3.15, s
18-OCH_3	58.9, CH_3	3.28, s				
N-CH_3	26.5, CH_3	2.82, s	26.4, CH_3	2.63, s	26.3, CH_3	2.78, s
3-OH		5.61, brs		6.06, brs		5.32, brs
7-OH		4.86, d (4.0)		4.85, d (5.5)		4.81, d (4.1)
12-NH		7.67, t (5.7)		7.67, t (5.5)		7.67, t (5.7)
16-OH				7.14, d (5.5)		
3′-OH		5.49, d (4.6)		5.47, d (4.8)		
7′-OH						4.90, d (5.3)

Table 2 ^{1}H NMR (600 MHz) and ^{13}C NMR (150 MHz) data for compounds **6a**/**6b** in CD_3OD

	6a		**6b**	
Position	δ_C, mult.	δ_H, mult. (J in Hz)	δ_C, mult.	δ_H, mult. (J in Hz)
1	183.3, C		182.6, C	
2	45.7, C		44.7, C	
3	81.4, CH	3.93, brs	83.5, CH	3.95, brs
4	87.7, C		86.0, C	
5	138.2, CH	5.89, d (14.5)	134.7, CH	6.01, dd (14.8, 2.6)
6	129.1, CH	6.27, m	129.7, CH	6.27, m
7	130.7, CH	6.27, m	131.1, CH	6.27, m
8	137.2, CH	5.80, dd (14.6, 6.4)	136.7, CH	5.77, dd (14.5, 6.4)
9	71.0, CH	4.43, q (6.4)	71.1, CH	4.43, q (6.4)
10	34.3, CH_2	2.94, dd (15.6, 6.2) 2.91, dd (15.6, 7.2)	34.3, CH_2	2.94, dd (15.6, 6.2) 2.91, dd (15.6, 7.2)
11	151.7, C		151.7, C	
12	124.0, CH	6.90, s	124.0, CH	6.90, s
13	152.6, CH	8.09, s	152.6, CH	8.08, s
14	20.4, CH_3	1.19, s	19.7, CH_3	1.04, s
15	26.2, CH_3	1.22, s	25.3, CH_3	1.21, s
16	22.0, CH_3	1.43, s	27.4, CH_3	1.49, s

(BGC-823), a large-cell lung carcinoma cell line (H460), a breast adenocarcinoma cell line (MDA-MB-231), and a hepatocellular carcinoma cell line (SMMC-7721). The cell lines were cultured in RPMI-1640 or DMEM medium supplemented with 10% heat-inactivated FBS. After incubation for 12 h, the cells were treated with compounds **1–2**, **4–6** at different concentrations (100, 33, 10, 3.3, 1.0, and 0.33 μM) for 48 h. The cytotoxic effects were assayed by the MTT method. Adriamycin was used as a positive control.

2.5. Cell cycle assay

SMMC7721 cells were seeded in 6-well plates with a density of 5 $\times$ 10^5 cells per well and treated with KSM-2690 B (**4**) (0 or 12.5 μM) for 24 h. The cells were then collected and fixed overnight in 75% ethanol at −20 °C. The next day, the cells were washed twice with cold PBS and gently resuspended in 500 μL propidium iodide (PI) working fluid (Dingguo Changsheng Biotechnology Co. Ltd., Beijing, China) and then incubated for 15 min in the dark at room temperature. Cell cycle analysis was performed by using a LSR-Fortessa flow cytometer with a collection of 20 000 cells. The population of cells in each phase was analyzed using ModFit LT 4.1 software (Verity Software House, Topsham, Me, USA). Each experiment was conducted three times.

2.6. Cell apoptosis assay

SMMC7721 cells were seeded in 6-well plates with a density of 5 $\times$ 10^5 cells per well and exposed to KSM-2690 B (**4**) (0 or 12.5 μM) for 24 h. Then, cells were collected, washed with cold PBS, and resuspended in 490 μL binding buffer and mixed with 5 μL of fluorescein isothiocyanate (FITC)-conjugated annexin-V reagent and 5 μL PI (BD, Franklin Lakes, NJ, USA). After 15 min incubation at room temperature in the dark, samples were analyzed by flow cytometry with the Annexin V-FITC/PI apoptosis method. Cytographs were presented by BD FACSDiva Software (BD, Franklin Lakes, NJ, USA). Each experiment was conducted three times.

2.7. Western blot analysis

SMMC 7721 cells were cultured in 6-well plates at a density of 5 $\times$ 10^5 cells per well for 12 h, and then treated with compound **4** (0, 6.25, 12.5, and 25 μM) for 24 h. After that, the cells were collected and lyzed by RIPA buffer and then extracted by protein extraction kits (Beyotime, Shanghai, China). The concentration of protein was determined by a BCA protein assay kits (Beyotime, Shanghai, China). Western blot analysis procedures were carried out as our previously described.[28] GAPDH expression was used as internal control. The GIS Gel Image System (Tanon, Shanghai, China) was used to quantitatively analyze the gray-scale of bands.

2.8. Data analysis

The results are presented as the mean ± standard deviation (SD) from at least three independent experiments. The differences of groups were analyzed using one-way analysis of variance with SPSS 13.0 (SPSS Inc., Chicago, IL, USA), followed by SNK (Student-Newman-Keuls) post hoc test. The threshold value for acceptance of difference was 5% ($p \leq 0.05$). The statistical analyses were performed using GraphPad Prism 5.0 (GraphPad Software, Inc., CA, USA).

3. Results and discussion

3.1. Isolation and structural elucidation

The 120 L fermentation broth of *S. glaucus* was clarified with a centrifuge to obtain a culture supernatant. The supernatant

was extracted by EtOAc three times. The combined EtOAc extract (32.7 g) were isolated by sequential column chromatography over silica gel, ODS, and MCI gel CHP-20P to yield oxazolomycins **1–6**.

Compound **1** was obtained as a yellow oil and its molecular formula was determined as $C_{37}H_{53}N_3O_{10}$ by HRESIMS at *m*/*z* [M + H]$^+$ 700.3738 and ^{13}C NMR data. The degrees of unsaturation of **1** was 13. The UV (λ_{max} 232 nm for a conjugated diene and λ_{max} 274 nm for a conjugated triene groups) and IR (ν_{max} 1820 cm^{-1} for a β-lactone andν_{max} 1677 cm^{-1} for a γ-lactam) spectra showed the typical characteristics of oxazolomycins.[1] The ^{1}H NMR (Table 1) data of **1** displayed the presence of two singlet aromatic heterocyclic hydrogens at δ_H 8.24, 6.90, nine olefinic hydrogens at δ_H 6.75, 6.41, 6.32, 6.12, 6.11, 5.93, 5.79, 5.61, and 5.60, four oxygenated methines at δ_H 4.95 (dd, J = 9.1, 2.4 Hz), 4.64 (d, J = 4.6 Hz), 3.83 (1H, m), 3.33 (1H, m), four methylenes including two methylenes bonded with heteroatom at δ_H 4.13 (dd, J = 12.0, 9.1 Hz), 3.99 (dd, J = 12.0, 2.4 Hz) and δ_H 3.71 (2H, m), two aliphatic methylenes at δ_H 3.55 (2H, d, J = 7.0 Hz), δ_H 1.96 (dt, J = 16.0, 6.5 Hz) and δ_H 1.12 (1H, m), two methines at δ_H 2.37, 1.59, two methoxyls at δ_H 3.28, 3.14, and six methyl groups including four singlet methyls at δ_H 2.82, 1.75, 1.09, 0.97 and two doublet methyls at δ_H 1.03, 0.86. In addition, four active hydrogens were observed at δ_H 7.67, 5.61, 5.49, 4.86. The ^{13}C NMR (Table 1) data of **1** exhibits 37 carbon signals, the type of these carbons were attributed to three carbonyls, three aromatic carbons, ten olefinic carbons, eight carbons bonded with heteroatom (four methines, two methylenes, and two carbons without directly bonded hydrogens), five aliphatic carbons (two methines, two methylenes, and one quaternary carbon), two methoxyls, and six methyls with the aid of HSQC experiment. The UV, IR, ^{1}H, and ^{13}C NMR data of **1** indicated it was a member of oxazolomycin family and was very similar to the known compound curromycin A.[6,7] The only difference between these two compounds was no substituent on oxazole moiety in **1** which was explained by the two singlet aromatic hydrogens at δ_H 8.24, 6.90 belonging to the oxazole. The planar structure of **1** was further confirmed by HMBC and ^{1}H–^{1}H COSY correlations (Fig. 2). The conjugated triene fragment was determined as 4′*Z*,6′*Z*,8′*E* according to the coupling constants $^3J_{H\text{-}6'/H\text{-}7'}$ = 11.3 Hz, $^3J_{H\text{-}8'/H\text{-}9'}$ = 14.5 Hz and NOE correlations between H-5′ (δ_H 6.41) and H_3-16′ (δ_H 1.75). Even though the geometry of conjugated diene could not confirmed by analysis the coupling constants of H-8/H-9 and H-10/H-11 because of the overlapped signals, the 8*Z*,10*Z* configurations could be determined by comparing the ^{1}H and ^{13}C NMR data with those of this family compounds.[10] The stereochemistry of characteristic oxazolomycins had been determined through X-ray crystallography and total synthesis experiments.[2,21–27] The stereochemistry of the spiro β-lactone-γ-lactam unit in natural oxazolomycins possessed 2*R*,3*S*,15*S*-configuration.[21–27] The configurations of the chirality carbons on the aliphatic chain of compound **1** were deduced as 4*S*,6*R*,7*R*,3′*R* based on the almost same ^{13}C NMR data of **1** with those of oxazolomycin A, lajollamycin, and synthesized oxazolomycins with the same side chain fragment.[21–27] The configuration of C-16 was suggested as 16*R* through analyzing the NOE correlations observed between 3-OH (δ_H 5.61) and H_2-18 (δ_H 4.13, 3.99), between H-16 (δ_H 4.95) and N-CH_3 (δ_H 2.82) (Fig. 3). Thus, the structure of **1** was elucidated and named oxazolomycin D.

Compound **2** was isolated as a yellow oil and possessed the molecular formula $C_{36}H_{51}N_3O_{10}$, as deduced by HRESIMS and ^{13}C NMR data, with 13 degrees of unsaturation. The ^{1}H and ^{13}C NMR (Table 1) data of **2** showed the feature of oxazole, triene, diene, and amide fragments which indicated **2** was a member of oxazolomycins. The NMR data of **2** was very similar to those of **1** except the methoxymethyl-β-lactone ring. Compared with **1**, the chemical shift of C-15, C-16, C-18 of **2** upshifted to δ_C 71.6, 69.9, 69.1, respectively and C-17 downshifted to δ_C 173.7. In addition, a methoxy was missing. These difference implied the methoxymethyl-β-lactone ring in **1** have changed. HMBC correlations between H_a-18 (δ_H 4.40) and C-15 (δ_C 71.6), C-17 (δ_C 173.7), and ^{1}H–^{1}H COSY correlations from H-16 (δ_H 4.83) to H-18 (δ_H 4.40, 4.17) indicated hydroxymethyl at C-16 and carbonyl at C-17

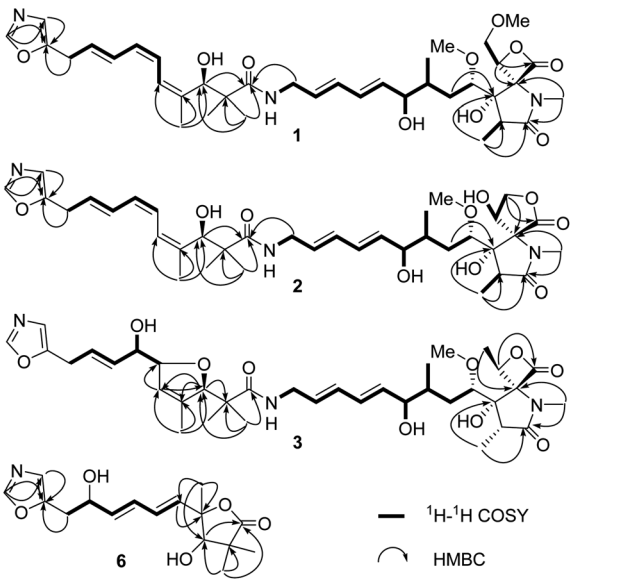

Fig. 2 Key HMBC and ^{1}H–^{1}H COSY correlations of compounds **1–3**, **6**.

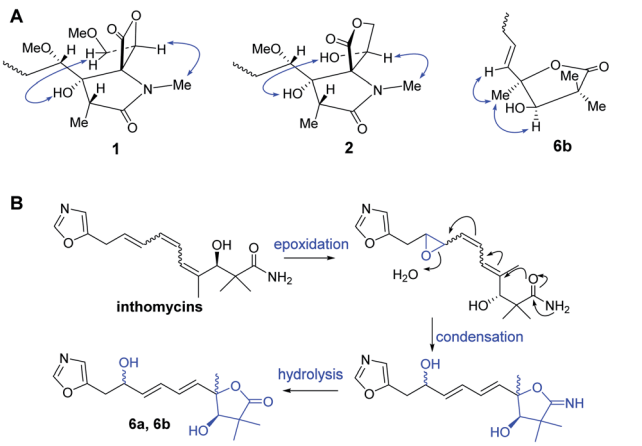

Fig. 3 (A) Key NOE correlations of compounds **1–2**, **6**; (B) proposed biosynthetic pathway of **6a** and **6b**.

forming a γ-lactone (Fig. 2). Moreover, the peaks at 1765 cm^{-1} and 1680 cm^{-1} in IR spectrum showed typical features of moieties of γ-lactone and γ-lactam in molecule. The same double-bond geometries as those of **1** were determined on the basis of ^1H–^1H coupling constants and NOE correlations. The 2*R*,3*S*,15*S* configuration of spiro fused γ-lactone-γ-lactam were suggested basis on the same biosynthesis reaction according to the ref. 29. NOE correlations observed between 3-OH (δ_H 6.06) and 16-OH (δ_H 7.14), between H-16 (δ_H 4.83) and N-CH_3 (δ_H 2.63) suggested the 16*R* configuration (Fig. 3). Identical ^{13}C NMR of aliphatic chain part of **2** with those of **1** showed they possessing the same configuration of C-4, C-6, C-7, C-3′. Therefore, **2** was determined and named oxazolomycin E.

Compound **3** was purified as a yellow oil. The molecular formula of **3** was determined to be $C_{36}H_{51}N_3O_{10}$ on the basis of HRESI mass spectrometry as well as ^1H and ^{13}C NMR data (Table 1). Interpretation of the ^1H, ^{13}C NMR and UV spectra suggested that **3** was also a congener of oxazolomycin and related to KSM-2690 B.[10] **3** differs from KSM-2690 B in the conjugated triene fragment. Four olefinic carbons at δ_C 138.4, 133.5, 125.5, 124.1 and two additional oxygenated methines at δ_C 88.5, 73.7 observed in the ^{13}C NMR spectrum of **3** suggested one double bond was oxygenated. The structure of **3** was partial changed during storage in the DMSO-d_6, and the 2D NMR appeared many disturbed signals. The definite ^1H–^1H COSY correlations from H-10′ (δ_H 3.40) to H-9′ (δ_H 5.68), from H-9′ (δ_H 5.68) to H-8′ (δ_H 5.53), from H-8′ (δ_H 5.53) to H-7′ (δ_H 3.89), from H-7′ (δ_H 3.89) to H-6′ (δ_H 4.51) and 7′-OH (δ_H 4.90) could confirmed the C-6′ and C-7′ were oxygenated. Even though there was no HMBC correlation found between H-3′ to C-6′ or between H-6′ to C-3′, a furan ring was formed through analysis the molecular formula and 13 degrees of unsaturation. The 2*R*,3*S*,4*S*,6*R*,7*R*,15*S*,16*S* were suggested through comparing the ^{13}C NMR data with those natural and synthesized congeners.[21–27] 3′*R* configuration was suggested on the basis of the biogenetic route and the configuration of C-6′ and C-7′ were undetermined. Thus, the structure of **3** was elucidated and named oxazolomycin F.

Compound **6a**/**6b** were obtained as a mixture of two epimers in a nearly 1.2 : 1 ratio, according to the integration of the ^1H NMR data. Their molecular formulas were established to be $C_{16}H_{21}NO_5$ by HRESIMS and ^{13}C NMR data. The signals of major isomer **6a** revealed that the presence of a oxazole (δ_C 152.6, 151.7, 124.0, δ_H 8.09, 6.90), a diene moiety (δ_C 138.2, 137.2, 130.7, 129.1, δ_H 6.27, 6.27, 5.89, 5.80), a α,α-dimethyl-β-hydroxy carbonyl group (δ_C 183.3, 81.4, 45.7, 26.2, 20.4, δ_H 3.93), a –CH_2CH(OH)- fragment (δ_C 71.0, 34.3, δ_H 4.43, 2.94, 2.91). The ^1H NMR and ^{13}C NMR data of **6a** showed typical characteristic of the structure motif of ozazolomycins and were very similar to those of inthomycins and phthoxazolins.[14,15] ^1H–^1H COSY established the fragment from H-5 to H-10 (Fig. 2). The conjugated diene fragment was determined as 5*E*,7*E* according to the coupling constants $^3J_{H\text{-}5/H\text{-}6}$ = 14.5 Hz, $^3J_{H\text{-}7/H\text{-}8}$ = 14.6 Hz. HMBC correlations from CH_3-14/15 (δ_H 1.22, 1.19) to C-1 (δ_C 183.3), C-2 (δ_C 45.7), C-3 (δ_C 81.4), from CH_3-16 (δ_H 1.43) to C-3 (δ_C 81.4), C-4 (δ_C 87.7), C-5 (δ_C 138.2), from H-5 (δ_H 5.89) to C-4 (δ_C 87.7) established the linkage of α,α-dimethyl-β-hydroxy carbonyl group and C-4, diene fragment and C-4. Even though there was no direct correlation evidence, a γ-lactone ring formed between C-1 and C-4 was deduced from the molecular formula and 7 degrees of unsaturation. This conclusion was further supported by the absorption peak observed at 1756 cm^{-1} in IR spectrum which revealed the typical characteristic of moieties of γ-lactone. The C-3 was suggested as *R* according to the same biosynthesis way as oxazolomycins and inthomycins. The only difference between **6a**/**6b** was the chemical shifts of Me-16 (δ_C 22.0 for **6a** and δ_C 27.4 for **6b**). Moreover, the different chemical shifts of C-3 ($\Delta\delta_{\mathbf{6a-6b}}$ −2.1), C-4 ($\Delta\delta_{\mathbf{6a-6b}}$ 1.7), C-5 ($\Delta\delta_{\mathbf{6a-6b}}$ 3.5) of **6a**/**6b** implied different configuration of C-4. The NOE correlations observed between H_3-16 (δ_H 1.49) and H-3 (δ_H 3.95), H-5 (δ_H 6.01) of **6b** suggested the methyl at C-4 was α-oriented in **6b**. Consequently, the methyl at C-4 was β in **6a**. Therefore, **6a** and **6b** were determined and named glaucumycins A and B, respectively. They were possibly derived from inthomycins in microorganisms by the proposed biosynthetic pathway in Fig. 3B.

3.2. Cytotoxic activity

Many members of oxazolomycin family showed cytotoxicities according to the ref. 2. The cytotoxic activities of compounds **1**–**2**, **4**–**6** against four human cancer cell lines were evaluated. The bioactive evaluation of **3** was not carried out because of the lack of material. As shown in Table 3, oxazolomycins **1**, **2**, **4**, **5** exhibited weak or moderate cytotoxic activity against the tested cancer cell lines, while compounds **6** was inactive at 100 μM. Compared with compound **2**, KSM-2690 B and C (**4**–**5**) showed stronger cytotoxicities. These results indicated the spiro fused β-lactone-γ-lactam core was quite favorable for the cytotoxic effect than γ-lactone-γ-lactam core (**4**, **5** *vs.* **2**). The methoxymethyl group at C-16 of β-lactone core was not benefit for its cytotoxic activity (**4** *vs.* **1**).

3.3. KSM-2690 B (4) caused SMMC 7721 cells S phase arrest

The ability to escape from controlled cell division is a hallmark of cancer. To investigate the possible molecular target resulting

Table 3 Cytotoxic (IC_{50} in μM) activities of compounds **1**–**2**, **4**–**6**

Compound	1	2	4	5	6	Adriamycin
BGC-823	89.5 ± 6.6	>100	36.7 ± 3.5	40.4 ± 5.2	>100	1.5 ± 0.1
H460	66.8 ± 3.4	75.6 ± 5.7	20.2 ± 1.6	34.8 ± 2.4	>100	1.0 ± 0.2
MDA-MB-231	80.2 ± 6.3	>100	10.6 ± 1.7	28.3 ± 2.3	>100	2.0 ± 0.4
SMMC7721	62.3 ± 4.5	78.1 ± 10.2	27.3 ± 2.1	43.2 ± 4.7	>100	2.2 ± 0.3

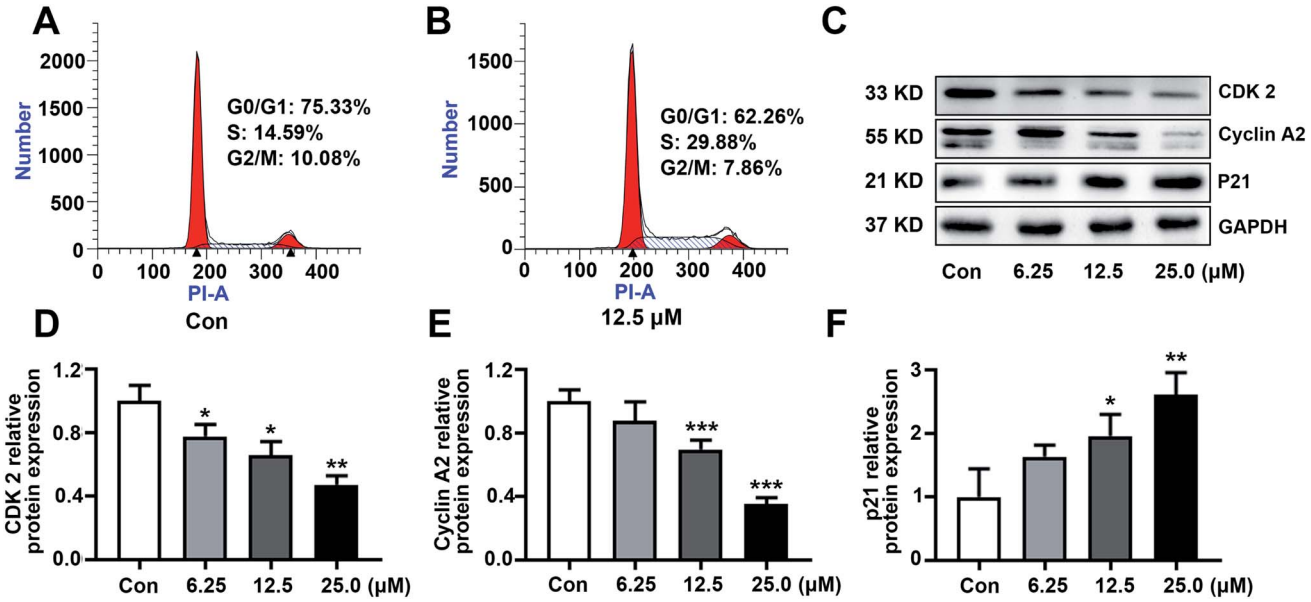

Fig. 4 KSM-2690 B (**4**) caused S phase cell cycle arrest in SMMC 7721 cells. (A and B) Cell cycle distribution were analyzed by flow cytometry in SMMC7721 cells treated with **4** (0 or 12.5 μM). (C) The protein levels of cyclin A2, CDK2, and p21 in SMMC7721 cells treated with KSM-2690 B (**4**) (6.25, 12.5, and 25 μM) were evaluated by western blot. (D–F) The relative quantities analysis of cyclin A2, CDK2, and p21 in SMMC7721 cells. *p < 0.05, **p < 0.01, and ***p < 0.001 *vs.* control.

in the cytotoxicity, the effect of KSM-2690 B (**4**) on cell cycle distribution was analyzed by flow cytometry. As shown in Fig. 4A and B, the percentage of SMMC7721 cells in S phase obviously increased after KSM-2690 B treatment. These results indicated that **4** caused S phase cell cycle arrest. As well known, cells through the different phases of cell cycle is regulated by specific cyclins and cyclin-dependent kinases (CDKs). CDK2 is activated by the binding of cyclin A and plays a key role throughout the S-phase in dividing cells.[30] At the same time, the up-regulation of the cyclin kinase inhibitor p21 have been reported to cause S phase cell-cycle arrest and its abnormal levels also influence the progress of DNA replication during cell-cycle progression at S phase. To further investigate the mechanism of **4** in S phase arrest, related S phase regulators cyclin A2, CDK2, and p21 were

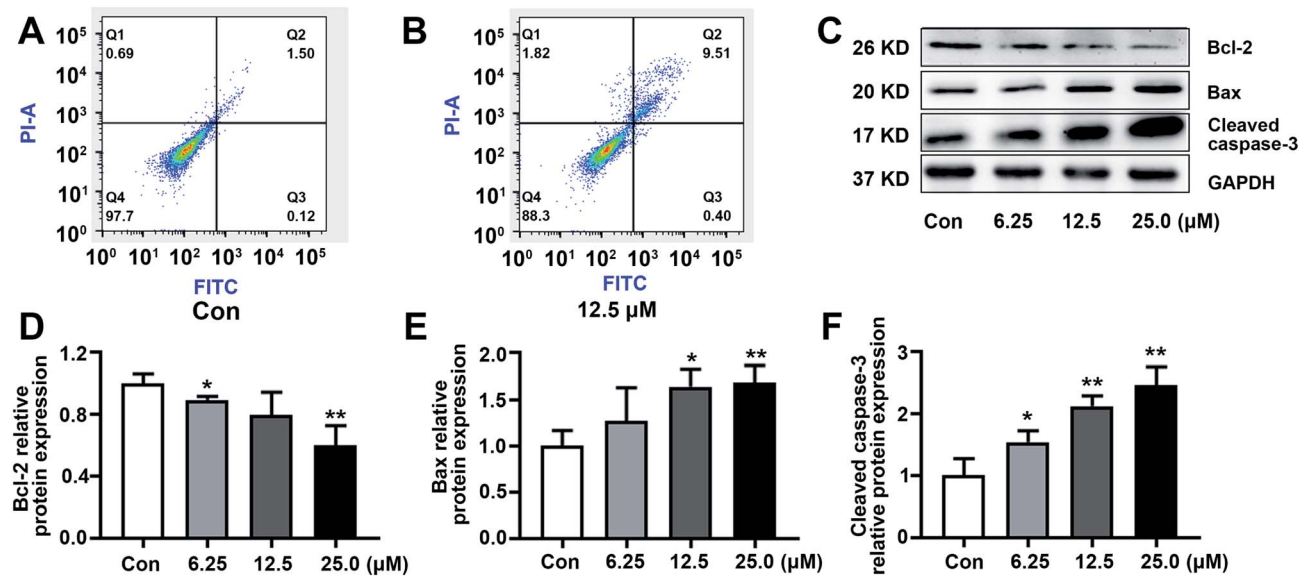

Fig. 5 KSM-2690 B (**4**) induced apoptosis in SMMC7721 cells. (A and B) KSM-2690 B (**4**) induced apoptosis was analyzed by flow cytometry in SMMC7721 cells treated with **4** (0 or 12.5 μM). (C) The protein levels of Bax, Bcl-2, and cleaved caspase-3 in SMMC7721 treated with KSM-2690 B (**4**) (6.25, 12.5, and 25 μM) were evaluated by western blot. (D–F) The relative quantities analysis of Bax, Bcl-2, and cleaved caspase-3 in SMMC7721 cells. *p < 0.05, **p < 0.01, and ***p < 0.001 *vs.* control.

examined by western blot method. As depicted in Fig. 4C–F, KSM-2690 B (**4**) decreased the protein levels of cyclin A2 and CDK2, and increased that of p21 in a dose-dependent manner.

3.4. KSM-2690 B (4) induced apoptosis in SMMC-7721 cells

To explore the effect of KSM-2690 B on apoptosis of SMMC7721 cells, apoptosis detection was carried out by flow cytometric assay. As shown in Fig. 5A and B, the population of apoptotic cells increased in **4**-treated SMMC7721 cells compared to the vehicle group. The results exhibited that **4** induced apoptosis in SMMC7721 cells. The balance of the pro-apoptotic factor Bax and anti-apoptotic factor Bcl-2 play an important role in progress of initiation of the apoptosis. The enhancement of Bax over Bcl-2 leads to the activation of caspases. The caspase-3 are crucial in the apoptosis cascade. Activation of executioner caspase-3, which results in cleaving structural proteins and causing the degradation of chromosomal DNA.[31] To further investigate the underlying mechanism of KSM-2690 B on apoptosis, the expression of key factors associated with apoptosis was examined by western blot. As shown in Fig. 5C–F, KSM-2690 B up-regulated the protein levels of Bax, whereas down-regulated that of Bcl-2 in SMMC7721 cells in a dose-dependent manner. In addition, the expression levels of cleaved caspase-3 was obviously increased compared to those of the vehicle group.

4. Conclusion

In summary, oxazolomycins D–F (**1–3**), a mixture of two isomers, glaucumycins A, B (**6a**/**6b**), as well as two known oxazolomycins (**4–5**) were isolated from *Streptomyces glaucus*. Oxazolomycins **1**, **2**, **4**, **5** demonstrated weak or modest cytotoxic activity against four human cancer cell lines, with IC_{50} values ranging from 10.6 ± 1.7 to 89.5 ± 6.6 μM (or >100 μM). Further study exhibited that **4** caused S phase cell cycle arrest and induced apoptosis in SMMC7721 cells through regulation the expression of related protein cyclin A2, CDK2, p21, Bcl-2, Bax, and activation the cleavage of caspase-3.

Conflicts of interest

The authors declare no competing financial interest.

Acknowledgements

This work was supported by Specific Research Project of Guangxi for Research Bases and Talents (grant no. AD18281066), P. R. China, and Science and Technology Major Project of Guangxi, P. R. China (grant no. AA18242026).

References

1 M. G. Moloney, P. C. Trippier, M. Yaqoob and Z. Wang, *Curr. Drug Discovery Technol.*, 2004, **1**, 181–199.
2 P. Oleksak, J. Gonda, E. Nepovimova, K. Kuca and K. Musilek, *RSC Adv.*, 2020, **10**, 40745–40794.
3 K. Takahashi, M. Kawabata, D. Uemura, S. Iwadare, R. Mitomo, F. Nakano and A. Matsuzaki, *Tetrahedron Lett.*, 1985, **26**, 1077–1078.
4 T. Mori, K. Takahashi, M. Kashiwabara, D. Uemura, C. Katayama, S. Iwadare, Y. Shizuri, R. Mitomo, F. Nakano and A. Matsuzaki, *Tetrahedron Lett.*, 1985, **26**, 1073–1076.
5 H. Kanzaki, K. Wada, T. Nitoda and K. Kawazu, *Biosci., Biotechnol., Biochem.*, 1998, **62**, 438–442.
6 M. Ogura, H. Nakayama, K. Furihata, A. Shimuza, H. Seto and N. Otake, *J. Antibiot.*, 1985, **38**, 669–673.
7 Y. Ikeda, S. Kondo, H. Naganawa, S. Hattori and M. Hamada, *J. Antibiot.*, 1991, **44**, 453–455.
8 G. Ryu, S. Hwang and S. Kim, *J. Antibiot.*, 1997, **50**, 1064–1067.
9 G. Ryu and S. Kim, *J. Antibiot.*, 1999, **52**, 193–197.
10 T. Otani, K. Yoshida, H. Kubota, S. Kawai, S. Ito, H. Horic, T. Ishiyama and T. Oki, *J. Antibiot.*, 2000, **53**, 1397–1400.
11 R. R. Manam, S. Teisan, D. J. White, B. Nicholson, J. Grodberg, S. T. C. Neuteboom, K. S. Lam, D. A. Mosca, G. K. Lloyd and B. C. M. Potts, *J. Nat. Prod.*, 2005, **68**, 240–243.
12 K. Ko, S. H. Lee, S. H. Kim, E. H. Kim, K. B. Oh, J. Shin and D. C. Oh, *J. Nat. Prod.*, 2014, **77**, 2099–2104.
13 W. Koomsiri, Y. Inahashi, T. Kimura, K. Shiomi, Y. Takahashi, S. Omura, A. Thamchaipenet and T. Nakashima, *J. Antibiot.*, 2017, **70**, 1142–1145.
14 Y. Tanaka, I. Kanaya, Y. Takahashi, M. Shinose, H. Tanaka and S. Omura, *J. Antibiot.*, 1993, **46**, 1208–1213.
15 K. Shiomi, N. Arai, M. Shinose, Y. Takahashi, H. Yoshida, J. Iwabuchi, Y. Tanaka and S. Omura, *J. Antibiot.*, 1995, **48**, 714–719.
16 S. Kawai, G. Kawabata, A. Kobayashi and K. Kawazu, *Agric. Biol. Chem.*, 1989, **53**, 1127–1133.
17 K. Kawazu, H. Kanzaki, G. Kawabata, S. Kawai and A. Kobayashi, *Biosci., Biotechnol., Biochem.*, 1992, **56**, 1382–1385.
18 H. Kanzaki, T. Ichioka, A. Kobayashi and K. Kawazu, *Biosci., Biotechnol., Biochem.*, 1996, **60**, 1535–1537.
19 E. O. Onyango, J. Tsurumoto, N. Imai, K. Takahashi, J. Ishihara and S. Hatakeyama, *Angew. Chem.*, 2007, **119**, 6823–6825.
20 J. H. Kim, I. Kim, Y. Song, M. J. Kim and S. Kim, *Angew. Chem.*, 2019, **131**, 11134–11138.
21 K. Eto, M. Yoshino, K. Takahashi, J. Ishihara and S. Hatakeyama, *Org. Lett.*, 2011, **13**, 5398–5401.
22 T. Nishimaru, K. Eto, K. Komine, J. Ishihara and S. Hatakeyama, *Chem.–Eur. J.*, 2019, **25**, 7927–7934.
23 M. Kumar, L. Bromhead, Z. Anderson, A. Overy and J. W. Burton, *Chem.–Eur. J.*, 2018, **24**, 1–5.
24 M. Yoshino, K. Eto, K. Takahashi, J. Ishihara and S. Hatakeyama, *Org. Biomol. Chem.*, 2012, **10**, 8164–8174.
25 J. P. N. Papillon and R. J. K. Taylor, *Org. Lett.*, 2000, **2**, 1987–1990.
26 S. Balcells, M. B. Haughey, J. C. L. Walker, L. Josa-Culleré, C. Towers and T. J. Donohoe, *Org. Lett.*, 2018, **20**, 3583–3586.
27 K. Eto, J. Ishihara and S. Hatakeyama, *Tetrahedron*, 2018, **74**, 711–719.

28 X. Gao, H. Yao, Y. Mu, P. Guan, G. Li, B. Lin, Y. Jiang, L. Han, X. Huang and C. Jiang, *Bioorg. Chem.*, 2019, **93**, 103311.
29 C. Zhao, J. M. Coughlin, J. Ju, D. Zhu, E. Wendt-Pienkowski, X. Zhou, Z. Wang, B. Shen and Z. Deng, *J. Biol. Chem.*, 2010, **285**, 20097–20108.
30 S. Tadesse, E. C. Caldon, W. Tilley and S. Wang, *J. Med. Chem.*, 2019, **62**, 4233–4251.
31 F. Edlich, *Biochem. Biophys. Res. Commun.*, 2018, **500**, 26–34.